

7-29-1998

Structural Study of $x\text{Na}_2\text{S} + (1 - x)\text{B}_2\text{S}_3$ Glasses and Polycrystals by Multiple-Quantum MAS NMR of ^{11}B and ^{23}Na

Sang-Jan Hwang
Iowa State University

C. Fernandez
Universite des Sciences et Technologies de Lille

Jean P. Amoureux
Universite des Sciences et Technologies de Lille

Jin-Woo Han
Taegu University

Jaephil Cho
Iowa State University

Follow this and additional works at: http://lib.dr.iastate.edu/mse_pubs

 *next page for additional authors*
Part of the [Ceramic Materials Commons](#), and the [Physical Chemistry Commons](#)

The complete bibliographic information for this item can be found at http://lib.dr.iastate.edu/mse_pubs/68. For information on how to cite this item, please visit <http://lib.dr.iastate.edu/howtocite.html>.

Structural Study of $x\text{Na}_2\text{S} + (1 - x)\text{B}_2\text{S}_3$ Glasses and Polycrystals by Multiple-Quantum MAS NMR of ^{11}B and ^{23}Na

Abstract

Glasses and polycrystals in the series $x\text{Na}_2\text{S} + (1 - x)\text{B}_2\text{S}_3$ have been prepared and studied by magic angle spinning (MAS) NMR and by two-dimensional multiple-quantum (MQ) MAS NMR of ^{11}B and ^{23}Na . These techniques, when applied at various magnetic fields and combined with computer simulations of the spectra, provide new insights into the structure of the polycrystalline samples. Isotropic chemical shifts, quadrupolar parameters, and relative concentrations of the various boron sites are obtained by NMR and correlated with the known structures of boron trisulfide ($x = 0$), sodium metathio borate ($x = 0.5$) and sodium orthothio borate ($x = 0.75$). A structural model of polycrystalline sodium dithio borate ($x = 0.33$) is proposed. The MQMAS NMR method significantly enhanced the resolution in ^{11}B spectra of $x\text{Na}_2\text{S} + (1 - x)\text{B}_2\text{S}_3$ glasses and proved instrumental in finding and identifying various structural units present within these materials as the modification of the B_2S_3 network progressed with increasing Na_2S content. The dominant ^{11}B resonances observed in the glassy samples represent the same basic structural units that were observed in the polycrystalline compounds. In addition, several new resonances featuring trigonally and tetrahedrally coordinated boron atoms in various transitional structures between dithio borate and metathio borate, or between metathio borate and orthothio borate, were found. ^{23}Na NMR proved less informative, especially in the glassy samples where the motion of the sodium ions between various sites precluded the observation of well-resolved spectra.

Keywords

Ames Laboratory

Disciplines

Ceramic Materials | Materials Science and Engineering | Physical Chemistry

Comments

Reprinted with permission from *Journal of the American Chemical Society* 120 (1998): 7337–7346, doi:10.1021/ja9800481. Copyright 1998 American Chemical Society.

Authors

Sang-Jan Hwang, C. Fernandez, Jean P. Amoureux, Jin-Woo Han, Jaephil Cho, Steve W. Martin, and Marek Pruski

Structural Study of $x\text{Na}_2\text{S} + (1 - x)\text{B}_2\text{S}_3$ Glasses and Polycrystals by Multiple-Quantum MAS NMR of ^{11}B and ^{23}Na

S.-J. Hwang,[†] C. Fernandez,[‡] J. P. Amoureux,[‡] J.-W. Han,[§] J. Cho,[⊥] S. W. Martin,[⊥] and M. Pruski^{*,†}

Contribution from Ames Laboratory, Ames, Iowa 50011, Laboratoire de Dynamique et Structure des Matériaux Moléculaires, CNRS URA 801, Université des Sciences et Technologies de Lille, F-59655 Villeneuve d'Ascq Cedex, France, Department of Physics, Taegu University, Kyungpook 713-714, Korea, and Department of Materials Science and Engineering, Iowa State University, Ames, Iowa 50011

Received January 5, 1998

Abstract: Glasses and polycrystals in the series $x\text{Na}_2\text{S} + (1 - x)\text{B}_2\text{S}_3$ have been prepared and studied by magic angle spinning (MAS) NMR and by two-dimensional multiple-quantum (MQ) MAS NMR of ^{11}B and ^{23}Na . These techniques, when applied at various magnetic fields and combined with computer simulations of the spectra, provide new insights into the structure of the polycrystalline samples. Isotropic chemical shifts, quadrupolar parameters, and relative concentrations of the various boron sites are obtained by NMR and correlated with the known structures of boron trisulfide ($x = 0$), sodium metathio borate ($x = 0.5$) and sodium orthothio borate ($x = 0.75$). A structural model of polycrystalline sodium dithio borate ($x = 0.33$) is proposed. The MQMAS NMR method significantly enhanced the resolution in ^{11}B spectra of $x\text{Na}_2\text{S} + (1 - x)\text{B}_2\text{S}_3$ glasses and proved instrumental in finding and identifying various structural units present within these materials as the modification of the B_2S_3 network progressed with increasing Na_2S content. The dominant ^{11}B resonances observed in the glassy samples represent the same basic structural units that were observed in the polycrystalline compounds. In addition, several new resonances featuring trigonally and tetrahedrally coordinated boron atoms in various transitional structures between dithio borate and metathio borate, or between metathio borate and orthothio borate, were found. ^{23}Na NMR proved less informative, especially in the glassy samples where the motion of the sodium ions between various sites precluded the observation of well-resolved spectra.

Introduction

Boron trisulfide (B_2S_3), also known as thio borate, is recognized as a strong glass-forming material and, like silica (SiO_2) and boron trioxide (B_2O_3), makes an excellent network former.¹ When incorporated with a network modifier, e.g., alkali sulfide (M_2S , $\text{M} = \text{Li}, \text{Na}, \text{K}, \text{Rb},$ and Cs), boron trisulfide forms binary glasses in a wide compositional range.² Despite stoichiometric similarities, there are notable structural distinctions between alkali thio borate and alkali borate glasses.³ Also, the replacement of oxygen with larger and more polarizable sulfur atom brings about significant increase in ionic conductivity, with the metallic ion M playing the role of a charge-conducting carrier.^{4–7} For example, several M_2S -based binary or ternary (with alkali halo sulfide, e.g., $\text{MI}-\text{M}_2\text{S}-\text{B}_2\text{S}_3$) thio borate glasses with room-temperature conductivity as high as $10^{-3} (\Omega\text{cm})^{-1}$ have been reported.⁷

In view of the potential utilization of thio borate glasses as solid-state electrolytes,^{1,4,7–11} it is important that their short-range order (SRO) structure be well understood.¹² One strategy used for such studies involves the systematic synthesis of structures with varying boron-to-sulfur ratio and correlating the compositional changes occurring with the evolution of infrared, Raman, or NMR spectra. Interpretation of the spectroscopic data can be assisted by the systematic X-ray characterization of those compounds that can form polycrystalline phase. For example, a review of thio compounds by Krebs¹³ includes several polycrystalline boron sulfides for which the crystal structures have been studied. These include B_2S_3 ,^{13,14} metathio borates ($\text{M}_3\text{B}_3\text{S}_6$, $\text{M} = \text{Na}, \text{K}, \text{Rb}$),^{13,15} and orthothio borates (M_3BS_3 , $\text{M} = \text{Na}, \text{Tl}$).^{16,17} Other well-characterized B–S systems include porphyrin-like molecular B_8S_{16} , one-dimensional

* To whom correspondence should be addressed.

[†] Ames Laboratory.

[‡] Université des Sciences et Technologies de Lille.

[§] Taegu University.

[⊥] Iowa State University.

(1) Martin, S. W.; Bloyer, D. R. *J. Am. Ceram. Soc.* **1990**, *73*, 3481.

(2) Cho, J. Ph.D. Thesis, Iowa State University, 1995.

(3) Sills, J. A.; Martin, S. W.; Torgeson, D. R. *J. Non-Cryst. Solids* **1996**, *194*, 260.

(4) Wada, H.; Menetrier, M.; Levasseur, A.; Hagenmuller, P. *Mater. Res. Bull.* **1983**, *18*, 189.

(5) Burckhardt, W.; Makyta, M.; Levasseur, A.; Hagenmuller, P. *Mater. Res. Bull.* **1984**, *19*, 1083.

(6) Pradel, A.; Ribes, M. *Mater. Sci. Eng.* **1989**, *B3*, 45.

(7) Kennedy, J. H.; Zhang, Z.; Eckert, H. *J. Non-Cryst. Solids* **1990**, *123*, 328.

(8) Martin, S. W.; Polewik, T. *J. Am. Ceram. Soc.* **1991**, *76*, 1466.

(9) Souquet, J. L.; Kone, A.; Levy, M. *Solid State Microbatteries*; NATO ASI Series; Akridge, J. R., Balkanski, M., Eds.; Plenum Press: New York, 1990; p 301.

(10) Ioyer, D. R.; Cho, J.; Martin, S. W. *J. Am. Ceram. Soc.* **1993**, *76*, 2753.

(11) Zhang, Z.; Kennedy, J. H.; Thompson, J.; Anderson, S.; Lathrop, D. A.; Eckert, H. *Appl. Phys.* **1989**, *A49*, 41.

(12) Hwang, S.-J.; Fernandez, C.; Amoureux, J. P.; Cho, J.; Martin, S. W.; Pruski, M. *Solid State Nucl. Magn. Reson.* **1997**, *8*, 109.

(13) Krebs, B. *Angew. Chem., Int. Ed. Engl.* **1983**, *22*, 113.

(14) Diercks, H.; Krebs, B. *Angew. Chem., Int. Ed. Engl.* **1977**, *16*, 313.

(15) Puttmann, C.; Diercks, H.; Krebs, B. *Phosphorus, Sulfur Silicon* **1992**, *65*, 1.

(16) Hagenmuller, P.; Chopin, F. C. R. *Hebdomadae Acad. Sci.* **1963**, *256*, 5578.

(17) Krebs, B.; Hamann, W. *J. Less-Comm. Met.* **1988**, *137*, 143.

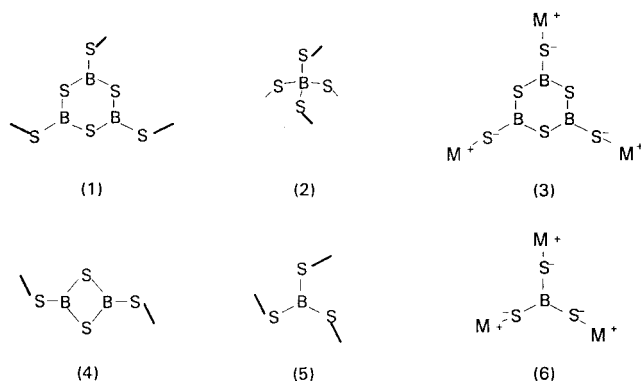


Figure 1. Proposed structural units found in alkali thioborate compounds: (1) thioboroxyl six-membered ring; (2) tetrahedral (BS_4) unit; (3) metathioborate; (4) four-membered ring; (5) trigonal (BS_3) unit; and (6) orthothioborate.

polymeric $(\text{BS}_2)_n$, and $\text{Pb}_2\text{B}_2\text{S}_5$ with tetrahedral BS_4 groups in adamantane-like $\text{B}_4\text{S}_{10}^{8-}$ anions.¹³ Figure 1 shows the structural units that are commonly found in alkali thioborate compounds.

The above strategy was used by Martin et al. in the IR studies of a wide range of the alkali thioborate glasses in the series $\text{M}_2\text{S}-\text{B}_2\text{S}_3$ ($\text{M} = \text{Li}, \text{Na}, \text{K}, \text{and Rb}$).^{1,10,18-21} These authors undertook the task of identifying the structural moieties at various glass composition ranges as mixtures of the structural phases known from the X-ray studies of crystalline compounds of similar composition. In some of these studies, traditional wide-line solid-state NMR was used to provide a quantitative measure of an N_4 fraction, which is the relative amount of tetrahedrally coordinated boron atoms in the sample.^{3,22} Similar studies were performed by Hintenlang et al.²³ on $\text{Li}_2\text{S}-\text{B}_2\text{S}_3$, Suh et al.²⁴ on $\text{Li}_2\text{S}-\text{LiI}-\text{B}_2\text{S}_3$, and Eckert et al. on $\text{Li}_2\text{S}-\text{P}_2\text{S}_5-\text{B}_2\text{S}_3$ ¹¹ and $\text{B}-\text{S}-\text{Ti}$.²⁵ On the basis of the static NMR spectra of polycrystalline and glassy phases and the N_4 fractions, structural models for various alkali thioborate glasses were proposed and compared with the structures established earlier for B_2O_3 -based compounds.

Still, the structural assignments proposed for these glasses and polycrystals are not complete. This is due to the inherent nonquantitative nature of vibrational spectroscopies, poor resolution of the traditional NMR methods, and difficulties in the preparation of high-purity samples. In this work, we present the results of a systematic study of the SRO structure of glasses and polycrystals in the series $x\text{Na}_2\text{S} + (1-x)\text{B}_2\text{S}_3$ using high-resolution solid-state NMR of ^{11}B and ^{23}Na . This study reports the well-resolved, isotropic spectra obtained with the recently developed two-dimensional MQMAS NMR technique.^{26,27} The MQMAS experiment correlates the evolution of symmetrical ($-m \leftrightarrow m$) multiple-quantum coherences in half-integer quadrupolar nuclei with the evolution of the central ($-1/2 \leftrightarrow 1/2$) transition under MAS to produce isotropic NMR spectra analogous to those obtained with double rotation (DOR)²⁸ and

dynamic angle spinning (DAS).²⁹ The technique offers a remarkable enhancement in resolution and proved instrumental in finding and identifying various structural units within the studied materials. Since the coherence transfer in the MQMAS experiment depends on the quadrupolar parameters and the crystallite orientation, the obtained intensities and line shapes differ from those in the standard, one-dimensional MAS spectra. Several strategies were proposed to achieve quantitative spectral intensities.^{12,27,30-32} For the polycrystalline samples, the approach used in this work is similar to that from our recent ^{11}B NMR study of vitreous boron trioxide ($v\text{-B}_2\text{O}_3$), polycrystalline boron trisulfide ($c\text{-B}_2\text{S}_3$), and vitreous boron trisulfide ($v\text{-B}_2\text{S}_3$).¹² The strategy relies upon the MQMAS experiments to obtain high-resolution and isotropic chemical shifts. This information is then used for simulation of the MAS spectra, acquired by using a short rf pulse to obtain the quadrupolar parameters and relative intensities. For most glassy samples, the quantitative measurements were limited to the N_4 fraction.

In addition, several ^{23}Na NMR experiments including MAS, MQMAS, and DOR are reported. Sodium, due to its relatively high sensitivity, 100% natural abundance, and moderate quadrupole coupling constant ($C_Q = e^2qQ/h$ is typically in the 1–3 MHz range), is very amenable to DOR, DAS, and MQMAS techniques; however, ^{23}Na NMR has rarely been used in the studies of glasses. This is mainly due to the high ionic mobility and inherent structural disorder, which result in relatively broad and featureless spectra.³³ This proved also to be the case in the $x\text{Na}_2\text{S} + (1-x)\text{B}_2\text{S}_3$ glasses. Nevertheless, for the polycrystalline samples, ^{23}Na NMR line shapes provided valuable information about the coordination of Na ions and their interaction with the bridging and nonbridging sulfide units.

Experimental Section

Sample Preparation. High-purity B_2S_3 is not available commercially. Therefore, the $v\text{-B}_2\text{S}_3$ used in this work as a starting material was synthesized in our laboratory following the method developed by Martin and Bloyer.¹ In this process, stoichiometric amounts of amorphous boron powder (Cerac, 99.9%, 3 μm particle size) and sulfur (Cerac, 99.999% 5 mm chunks) were reacted under vacuum at 850 $^\circ\text{C}$ in sealed, carbon-coated silica tubes in a furnace rotating at 5 rpm. Polycrystalline B_2S_3 was obtained by heat treating the $v\text{-B}_2\text{S}_3$ at 450 $^\circ\text{C}$ in a similar carbon-coated silica tube for approximately two weeks, grinding the obtained product, and repeating the annealing process.

The $x\text{Na}_2\text{S} + (1-x)\text{B}_2\text{S}_3$ samples were prepared by melting a mixture of Na_2S (Cerac, 99.9%) and $v\text{-B}_2\text{S}_3$ powders in a carbon crucible for 15 min at 850 $^\circ\text{C}$. Glasses were prepared by rapid quenching between stainless steel plates. Three compositions of $x\text{Na}_2\text{S} + (1-x)\text{B}_2\text{S}_3$ polycrystals, $x = 0.33, 0.5,$ and 0.75 , were synthesized by solid-state reactions of stoichiometric amounts of $v\text{-B}_2\text{S}_3$ and Na_2S in carbonized quartz tubes at 500 to 550 $^\circ\text{C}$ over a period of 1 week. The resulting sample materials were crushed into a fine powder. These samples will be referred to as dithioborate ($\text{Na}_2\text{S}\cdot 2\text{B}_2\text{S}_3$, $x = 0.33$), metathioborate ($\text{Na}_2\text{S}\cdot \text{B}_2\text{S}_3$, $x = 0.50$), and orthothioborate ($3\text{Na}_2\text{S}\cdot \text{B}_2\text{S}_3$, $x = 0.75$). The formation of polycrystalline and glassy phases was verified by X-ray diffraction.

Because the $x\text{Na}_2\text{S} + (1-x)\text{B}_2\text{S}_3$ samples are extremely hygroscopic, their preparation and handling were carried out in a glovebox with a dried helium gas atmosphere (H_2O and O_2 concentration less

(18) Martin, S. W.; Bloyer, D. R. *J. Am. Ceram. Soc.* **1991**, *74*, 1003.
 (19) Cho J.; Martin S. W. *J. Non-Cryst. Solids* **1994**, *170*, 182.
 (20) Cho J.; Martin S. W. *J. Non-Cryst. Solids* **1995**, *182*, 248.
 (21) Cho J.; Martin S. W. *Phys. Chem. Glasses* **1995**, *36*, 239.
 (22) Sills, J. A.; Martin, S. W.; Torgeson, D. R. *J. Non-Cryst. Solids* **1994**, *168*, 86.
 (23) Hintenlang, D. E.; Bray, P. J. *J. Non-Cryst. Solids* **1985**, *69*, 243.
 (24) Suh, K. S.; Hojjaji, A.; Villeneuve, G.; Menetrier, M.; Levasseur, A. *J. Non-Cryst. Solids* **1991**, *128*, 13.
 (25) Eckert, H.; Muller-Warmuth, W.; Hamann, W.; Krebs, B. *J. Non-Cryst. Solids* **1984**, *65*, 53.
 (26) Frydman, L.; Harwood, J. S. *J. Am. Chem. Soc.* **1995**, *117*, 5367.
 (27) Medek, A.; Harwood, J. S.; Frydman, L. *J. Am. Chem. Soc.* **1995**, *117*, 12779.

(28) Samoson, A.; Sun, B.; Pines, A. *Mol. Phys.* **1988**, *65*, 1013.
 (29) Mueller, K. T.; Sun, B.; Chingas, G. C.; Zwanziger, J. W.; Terao, T.; Pines, A. *J. Magn. Reson.* **1990**, *86*, 470.
 (30) Fernandez, C.; Amoureux, J. P.; Chezeau, J. M.; Delmotte, L.; Kessler, H. *Microporous Mater.* **1996**, *6*, 331.
 (31) Wu, G.; Rovnyank, D.; Sun, B.; Griffin, R. G. *Chem. Phys. Lett.* **1996**, *249*, 210.
 (32) Massiot, D.; Touzo, B.; Trumeau, D.; Coutures, J. P.; Virelet, J.; Florian, P.; Grandinetti, P. *J. Solid State Nucl. Magn. Reson.* **1996**, *6*, 73.
 (33) Xue, X.; Stebbins J. F. *Phys. Chem. Miner.* **1993**, *20*, 297.

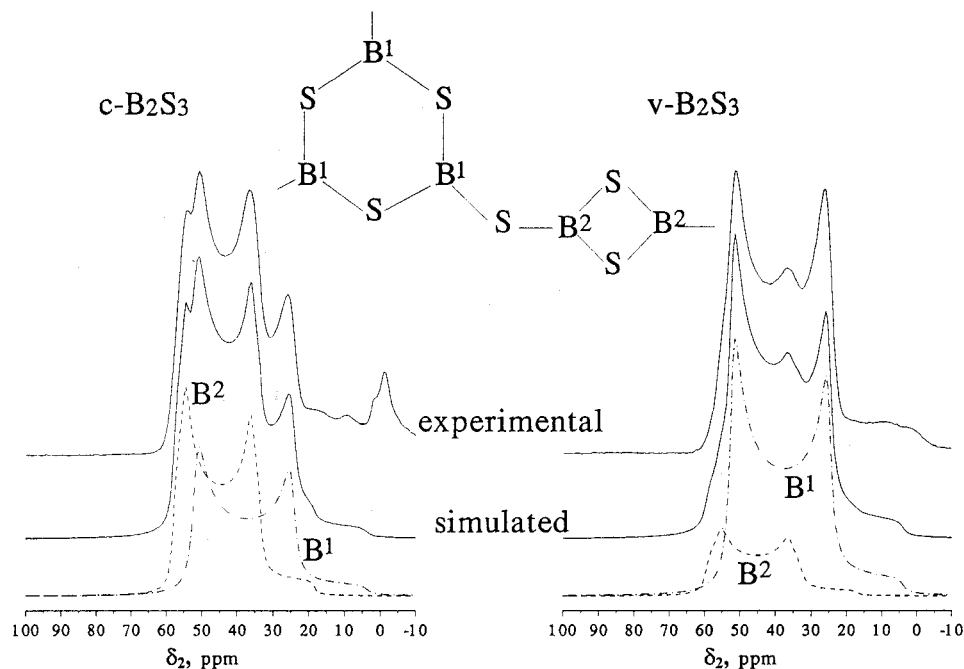


Figure 2. ^{11}B MAS NMR spectra of polycrystalline and glassy B_2S_3 at 5.9 T and the corresponding simulated line shapes. Only the resonances located between 20 and 60 ppm were included in the simulations.

than 2 ppm). However, the NMR experiments show that some contamination with oxygen did occur during the synthesis and/or handling of the starting material ($v\text{-B}_2\text{S}_3$) and the derived compounds. The NMR fingerprints of the structural units that resulted from the presence of oxygen in $v\text{-B}_2\text{S}_3$ were described in detail elsewhere.¹²

NMR Measurements. One-dimensional MAS NMR spectra of ^{11}B and ^{23}Na were obtained at 4.7, 5.9, 8.5, and 9.4 T on home-built NMR spectrometers equipped with home-built MAS NMR probes. A 5 mm rotor was filled with a sample in a glovebox and spun at 8 to 10 kHz, which sufficed to remove the spinning sidebands from the central portion of the spectrum. The rotor cap fits tightly inside the rotor body to minimize the oxygen contamination of samples during the MAS experiments. A single rf pulse corresponding to a $\sim 20^\circ$ tip angle in a liquid was found adequate for obtaining accurate ^{11}B and ^{23}Na intensities in various structural environments.

The MQMAS NMR of ^{11}B and ^{23}Na were performed at 9.4 T on a Bruker ASX 400 spectrometer equipped with a 4 mm Bruker MAS probe. The radio frequency power used was sufficient to produce a selective $\pi/2$ pulse in 0.8–0.9 s for these $\text{spin-}3/2$ nuclei. Excitation of both the echo ($-3Q$) and antiecho ($+3Q$) coherences was achieved by using a simple two-pulse (preparation and mixing) sequence described elsewhere.³⁴ The 6-phase cycling scheme used to simultaneously select $3Q$ coherence pathways was combined with classical CYCLOPS to eliminate receiver artifacts and with a 12-phase TPPI cycling scheme to produce pure-phase 2D spectra.^{12,34} The 2D spectra are presented in the figures after the shearing transformation.

In the MAS spectra reported in this work, only the centerband corresponding to the central transition spectrum is shown. All NMR shifts in the MAS and MQMAS spectra are reported with use of the δ scale,³⁵ with positive values being downfield, and are referenced to $\text{BF}_3\cdot\text{O}(\text{C}_2\text{H}_5)_2$ for ^{11}B and to a 0.1 mol aqueous solution of NaCl for ^{23}Na . Within the text, the resonance positions are expressed in terms of the chemical shifts CS, which differ from the frequencies observed in the spectra due to the presence of the quadrupolar-induced shifts. The quadrupolar parameters and isotropic chemical shift were obtained directly from the 2D MQMAS spectra and/or from the 1D MAS spectra by using the simulation program, QUASAR.³⁶

Results and Discussion

1. ^{11}B NMR. A detailed NMR analysis of the $c\text{-B}_2\text{S}_3$ and $v\text{-B}_2\text{S}_3$ samples was recently described in a separate publication.¹² However, since the same $v\text{-B}_2\text{S}_3$ material was used to produce the glasses studied in the present work, a brief summary of these earlier results is given below. Also, the discussion on the structural chemistry of $x\text{Na}_2\text{S} + (1-x)\text{B}_2\text{S}_3$ glasses will be preceded by the analysis of three types of $x\text{Na}_2\text{S} + (1-x)\text{B}_2\text{S}_3$ polycrystals prepared for this work. This information proved instrumental in monitoring the chemical evolution of the glassy samples, which often exhibited spectroscopic evidence of being a mixture of these basic structures.

1.1. Polycrystalline and Vitreous B_2S_3 . The ^{11}B MAS NMR spectra of $c\text{-B}_2\text{S}_3$ and $v\text{-B}_2\text{S}_3$ taken at 5.9 T and their corresponding simulated line shapes are shown in Figure 2.

The central portions of both spectra are a superposition of (at least) two second-order quadrupolar powder patterns representing trigonally coordinated boron sites, which are referred to as B^1 and B^2 .¹² For both the polycrystalline and vitreous samples, the computer simulations of the spectra in Figure 2 and of similar spectra obtained at 4.7, 8.5, 9.4, and 14.1 T (not shown) yielded consistent results for the isotropic chemical shift δ_{CS} (61 and 64 ppm, respectively, for B^1 and B^2), the quadrupolar coupling constant C_Q (2.40 and 2.15 MHz), and the asymmetry parameter η_Q (0.05 and 0.13).¹² On the basis of the isotropic chemical shifts,³⁷ the B^1 and B^2 resonances were assigned to boron atoms in six-membered (borosulfol) rings and four-membered rings, respectively [structures **1** and **4** in Figure 1]. These results represent the strongest spectroscopic evidence of the presence of two distinct BS_3 environments since the X-ray crystal structure of B_2S_3 was reported by Diercks and Krebs two decades ago.¹⁴ While δ_{CS} , C_Q , and η_Q were identical for the glassy and crystal structures, the relative intensities obtained by integrating the B^1 and B^2 resonances, including the spinning sidebands (not shown), differed considerably. According to the

(34) Fernandez, C.; Amoureux, J. P. *Chem. Phys. Lett.* **1995**, *242*, 449.

(35) Amoureux, J. P.; Fernandez, C. *Solid State Nucl. Magn. Reson.* **1998**, *10*, 211.

(36) Amoureux, J. P.; Fernandez, C.; Dumazy, Y. 37th Rocky Mountain Conference, Denver, 1995, Abstract No. 264.

(37) Noth, H.; Wrackmeyer, B. Nuclear Magnetic Resonance Spectroscopy of Boron Compounds. In *NMR Basic Principles and Progress*; Diehl, P., Fluck, E., Kosfeld, R., Eds.; Springer-Verlag: Berlin, 1978; Vol. 14.

X-ray study, the boron atoms in six- and four-membered rings should exhibit a 3:1 intensity ratio. This agrees well with the results for the vitreous sample (3.8:1); however, a B¹:B² intensity ratio of 2:3 was measured for our c-B₂S₃ sample.¹² Clearly, our c-B₂S₃ sample differs significantly from the crystal described in Krebs' work.¹⁴ This was, at least in part, explained by the 2D-MQMAS experiment, which showed the presence of well-resolved resonances assigned to BS₂O, BSO₂, BO₃, and BS₄ units existing within this sample. By using the spectral information from the MQMAS experiment, the 1D MAS spectra of c-B₂S₃ were integrated to yield the relative concentrations of boron atoms in the various environments.¹² The above structural model for v-B₂S₃ is quite different than that for v-B₂O₃, where the structure is proposed to consist of six-membered (boroxol) rings linked by and "loose" BO₃ triangles.¹² While the presence of four-membered rings in the v-B₂S₃ sample was implied on the basis of the similarity of its MQMAS spectrum to that measured for c-B₂S₃, the structural model involving "loose" BS₃ triangles in v-B₂S₃ cannot be ruled out without further study of this system.³⁸

1.2. Polycrystalline Phases. The $x\text{Na}_2\text{S} + (1 - x)\text{B}_2\text{S}_3$ polycrystals prepared in this work were discovered earlier. The metathiorborate and orthothiorborate phases were reported in the 1960s by Chopin et al.³⁹ and by P. Hagenmuller et al.,¹⁶ respectively. Their structures consist of six-membered rings and of isolated Na₃BS₃ units, respectively, as depicted in Figure 1. The dithiorborate phase was reported in a recent study of this system with static ¹¹B NMR but its structure was not resolved.²²

The formation of polycrystalline phases was verified by using X-ray diffraction, and was also confirmed by the presence of sharp features in the ¹¹B MAS spectra and increased longitudinal magnetic relaxation times. The ¹¹B MAS NMR spectra of these three samples were taken at 4.7, 5.9, 8.5, and 9.4 T. Those obtained at 5.9 T and the corresponding line shape simulations are shown in Figure 3a. The ¹¹B MQMAS spectra of Na₂S·B₂S₃ and 3Na₂S·B₂S₃ polycrystalline samples measured at 9.4 T are presented in Figures 3b and 3c, where δ_2 and δ_{ISO} represent the MAS (single-quantum) and the isotropic (triple-quantum) dimensions, respectively. The NMR results demonstrate the extensive structural evolution that the $x\text{Na}_2\text{S} + (1 - x)\text{B}_2\text{S}_3$ compounds undergo as the concentration of Na₂S increases. Below, we will examine these changes in detail.

1.2.1. Na₂S·2B₂S₃. The MAS spectrum of polycrystalline Na₂S·2B₂S₃ (Figure 3a, bottom trace) shows a narrow peak that is characteristic of boron sites in a symmetric local environment. A computer simulation of this spectrum revealed the presence of two components at $\delta_{\text{CS}} \approx -1.5$ ppm (representing 78(5)% of sites) and $\delta_{\text{CS}} \approx -3$ ppm (representing the remaining 22-(5)% of the total intensity), with a small C_Q value of 0.8(0.05) MHz. This indicates that all boron atoms, which occupied trigonal sites in B₂S₃, are now located in tetrahedral BS₄ units (referred to as B³) with negligible EFG. A similar result was observed earlier in our laboratories with use of static ¹¹B NMR.²² This remarkable conversion of trigonal groups to tetrahedral

boron groups seems unique for the boron sulfide system. In particular, the structural chemistry of Na₂S₂B₂S₃ must differ significantly from that of the binary sodium borate crystal with diborate composition (Na₂O·2B₂O₃), where 50% of boron atoms remain trigonally coordinated.^{40,41} On the basis of the ¹¹B MAS spectrum, we conclude that the crystal structure of Na₂S·2B₂S₃ consists of adamantane-like B₄S₆ units that are coupled via shared, tetrahedrally coordinated S atoms and via four S bridges, as depicted in Figure 4. The existence of two distinct tetrahedral sites in this sample is difficult to explain. The presence of Na⁺ cations, which are relatively mobile (see the discussion of ²³Na NMR data given below) and most likely are distributed over several partially occupied sites along the channels, may be responsible for this effect. This unusual tetrahedral coordination of boron was observed earlier in several thiorborates, e.g., Pb₄B₄S₁₀ (4PbS·2B₂S₃), Ag₆B₁₀S₁₈ (3Ag₂S·5B₂S₃), and Li₈[B₁₀S₁₈]S_x (LiBS₂).^{13,42}

1.2.2. Na₂S·B₂S₃. Another structural change occurs when the Na₂S content is increased to $x = 0.5$. The ¹¹B MAS NMR spectrum of polycrystalline Na₂S·B₂S₃ (Figure 3a, middle trace) shows that nearly all boron atoms are once again trigonally coordinated. The isotropic chemical shift δ_{CS} obtained from the analysis of the MQMAS spectrum of Figure 3b and from the spectral simulation of the main feature of the MAS spectrum of Figure 3a is ~ 60 ppm. Within experimental error, this value is equal to the δ_{CS} value observed for the BS₃ units in the six-membered rings of B₂S₃. The corresponding C_Q values are also similar: 2.42 (0.05) MHz vs 2.40 (0.05) MHz in B₂S₃. However, the boron atoms in Na₂S·B₂S₃ appear to be located in a more asymmetric EFG, as the best fit of the observed MAS powder pattern was obtained for $\eta_Q = 0.43(0.04)$. These results are consistent with the structural unit of metathiorborate shown in Figure 1 and with the crystal structure that was proposed earlier for this compound based on the X-ray diffraction studies.^{13,15} The increased asymmetry parameter and the corresponding distorted powder pattern can be explained by the presence of the negatively charged sulfur atoms on the outside of the metathiorboroxyl (B₃S₆³⁻) rings.

The computer simulations were performed only for the one type of trigonally coordinated boron that dominates the NMR spectrum. However, as we showed previously,¹² the less abundant structural units present in this sample exhibit overlapping resonances in the 1D MAS spectra, but are well resolved by the MQMAS technique. Besides the resonance from the B₃S₆³⁻ rings (denoted B⁴ in Figure 3b), the following resonances can be distinguished in the isotropic (δ_{ISO}) dimension of the MQMAS spectrum:

(i) Resonance B³ at ~ 0 ppm, which is assigned to the BS₄ units, most likely results from the presence of residual dithiorborate.

(ii) We have shown in our earlier work on the structure of B₂S₃¹² that the two resonances at $\delta_{\text{CS}} \approx 17$ ppm and at $\delta_{\text{CS}} \approx 44$ ppm are attributed to BO₃ and BS₂O units, respectively. Although the combined intensity of these two resonances does not exceed a few percent of the total signal, their presence shows that some inclusion of oxygen occurred during the synthesis and/or handling of the samples. The BO₃ units could not be identified in the standard ¹¹B MAS spectra, because their resonance overlaps with that of BS₄ sites (B³) in the anisotropic spectrum.

(iii) The numerical simulations of the MAS spectrum of Figure 3a, for $x = 0.50$, revealed that the feature located between

(38) We note that further studies of well-crystallized thiorborate compounds of higher purity are needed to better establish the identity of the BS₃ species described in ref 12. Another probable scenario has been recently brought to our attention, which assumes that the sample labeled c-B₂S₃ was a mixture of crystalline BS₂ and glassy B₂S₃. Such units were found previously in crystalline BS₂ with wide-line ¹¹B NMR see: Hurter, H. U.; Krebs, B.; Eckert, H.; Muller-Warmuth, W. *Inorg. Chem.* **1985**, *24*, 1288), and their quadrupolar parameters match those of the B² sites identified in ref 12. Similarly, the ratio of 3.8:1 between B¹ and B² sites in our v-B₂S₃ sample could be due to the presence of a small concentration of the BS₂ units in the glassy structure.

(39) Chopin, F.; Turnell, G. *J. Mol. Struct.* **1969**, *3*, 57.

(40) Krogh-Moe, J. *Acta Crystallogr.* **1962**, *15*, 190.

(41) Krogh-Moe, J. *Acta Crystallogr.* **1968**, *B24*, 179.

(42) Hebel, P. Z.; Krebs, B.; Grune, M.; Muller-Warmuth, W. *Solid State Ionics* **1990**, *43*, 133.

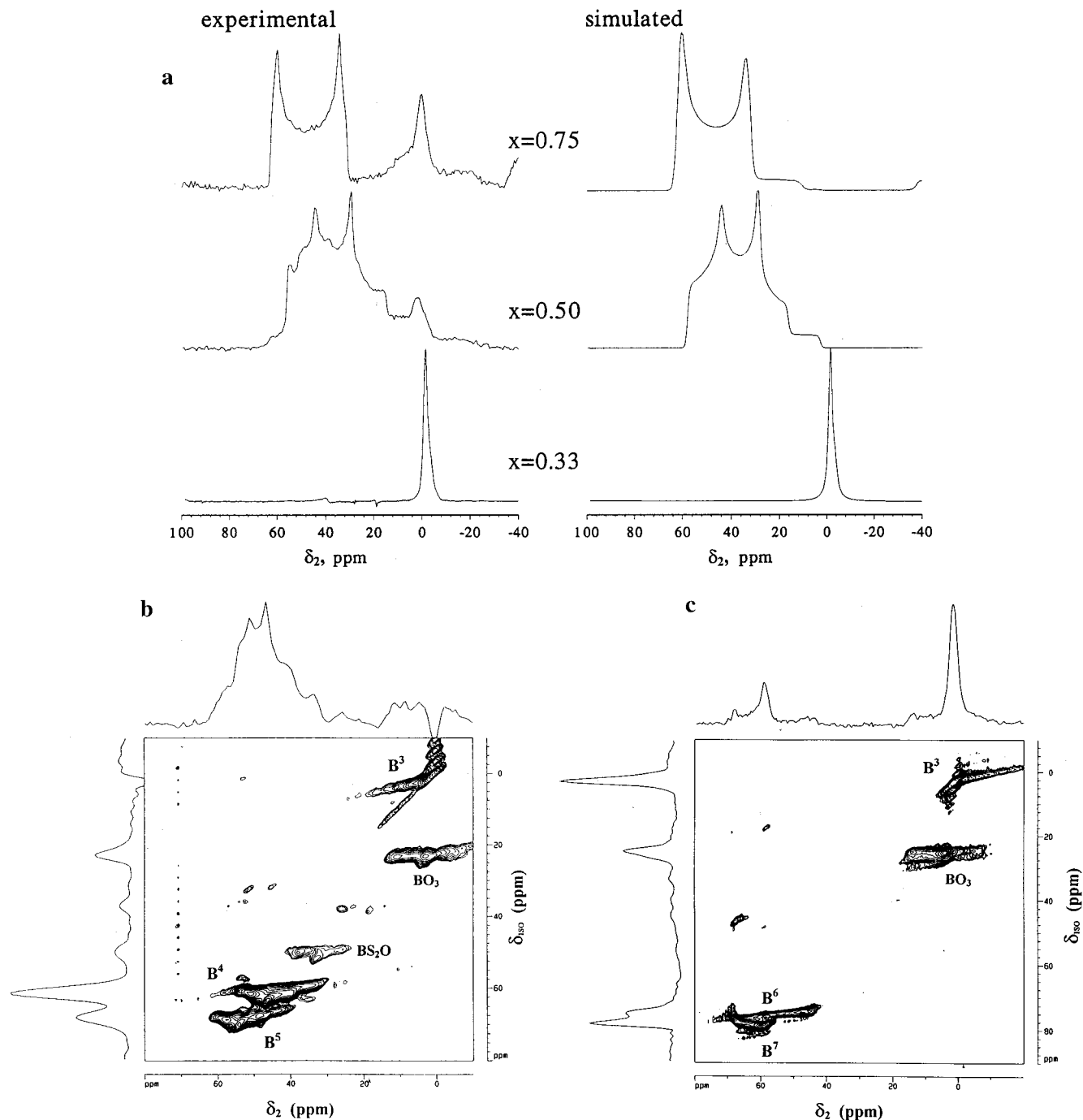


Figure 3. (a) Experimental and simulated ^{11}B MAS NMR spectra of polycrystalline samples: dithiorate ($x = 0.33$), metathiorate ($x = 0.50$), and orthothiorate ($x = 0.75$) at 5.9 T. Spectra b and c were taken at 9.4 T with metathiorate and orthothiorate, respectively, using ^{11}B MQMAS NMR.

20 and 60 ppm, which mostly represents the BS_3 units in metathioroxyl rings $\text{B}_3\text{S}_6^{3-}$, includes a small contribution from a second type of BS_3 species. The existence of another BS_3 site became evident in the MQMAS spectrum of Figure 3b, where it is labeled as B^5 . This resonance has a chemical shift of ~ 64 ppm and most likely represents a trigonal boron site in a unit that is a transitional form between dithiorate and metathiorate [e.g. $(\text{Na}^+\text{S}^-)_2\text{B}-\text{S}-\text{B}_3\text{S}_6$], or between metathiorate and orthothiorate [e.g. pyrothiorate $(\text{Na}^+\text{S}^-)_2\text{B}-\text{S}-\text{B}(\text{S}^-\text{Na}^+)_2$].

1.2.3. $3\text{Na}_2\text{S}\cdot\text{B}_2\text{S}_3$. The ^{11}B MAS and MQMAS spectra of $3\text{Na}_2\text{S}\cdot\text{B}_2\text{S}_3$ are shown in Figures 3a (top trace) and 3c, respectively. The downfield portion of the MAS spectrum could be reasonably well fit assuming the presence of a single BS_3^{3-}

site located in an environment with a highly symmetric EFG. The presence of BS_3^{3-} units (see structure 6 in Figure 1) is consistent with the structure of orthothiorate, which is expected for this composition.^{16,17} However, the MQMAS spectrum revealed the existence of two similar sites B^6 and B^7 with δ_{CS} values of 67 and 71 ppm, respectively. A possible explanation of this result is that distinct BS_3^{3-} units exist in this sample due to the presence of two differently coordinated Na^+ ions. This scenario will be discussed later with ^{23}Na MAS NMR results. Small concentrations of tetrahedral BS_4 (B^3) sites and trigonal BO_3 sites were also found in this sample.

1.3. Low Alkali Glasses ($x = 0.33$). Figure 5a shows the ^{11}B MAS NMR spectra of $x\text{Na}_2\text{S} + (1-x)\text{B}_2\text{S}_3$ glasses for $0 \leq x \leq 0.33$. In Figure 5b the same results are replotted in order

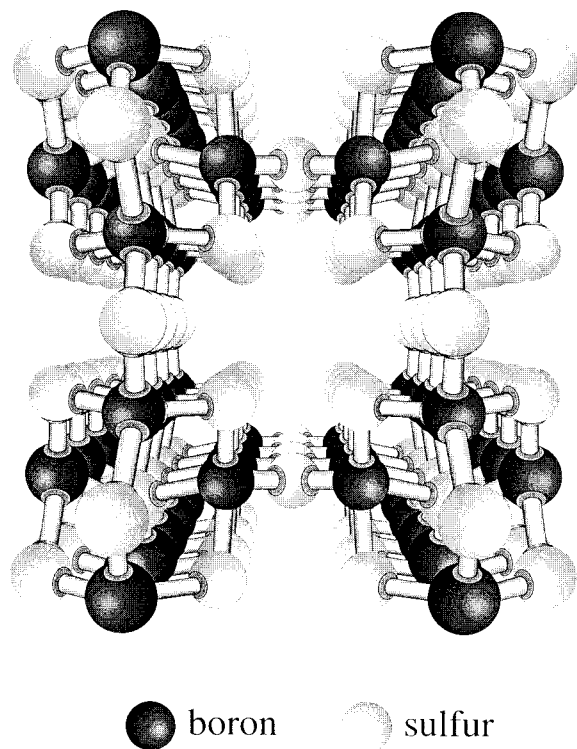


Figure 4. Adamantane-like structure of $\text{Na}_2\text{S}_2\text{B}_2\text{S}_3$. The sodium cations (not shown) are most likely distributed along the channels.

to highlight the spectral region between 20 and 60 ppm. The spectra demonstrate progressive evolution of the glass structure from $v\text{-B}_2\text{S}_3$ to one that consists primarily of tetrahedrally coordinated boron atoms. The observed shift and line shape of the narrow peak at $\delta_{\text{CS}} \approx 0$ ppm are consistent with that observed for dithioborate, as discussed above (see Figure 3a). We note that the conversion rate of BS_3 into BS_4 units is rapid for $0 \leq x \leq \sim 0.15$, but tapers off when x exceeds 0.15. In contrast to the polycrystalline sample, the conversion is not complete for the glass at $x = 0.33$. Still, the maximum N_4 fraction measured (~ 0.75) exceeds by a factor of almost two the values reported for the $x\text{Na}_2\text{O} + (1-x)\text{B}_2\text{O}_3$ glasses.^{43,44} Other conclusions that result from the spectra of Figure 5 can be summarized as follows:

(i) Figure 5b shows that the creation of BS_4 sites does not have a significant effect on the symmetry of the adjacent trigonal sites as their line shape remains unchanged with the increasing sodium sulfide content. Furthermore, there is no noticeable change in the line shift of this resonance with increasing Na_2S content. The presence of such a shift would not be surprising for those thioboroxyl rings that are linked to BS_4 units.

(ii) A numerical analysis of the two superimposed powder patterns from the six-membered rings and the four-membered rings revealed that their intensity ratio remains approximately constant in the whole range $0.075 \leq x \leq 0.33$. Again this is somewhat surprising, as the four-membered rings have more strain on the ring bonds, and should be more amenable to structural change.

(iii) Finally, we note the emergence of a weak shoulder at $\delta_{\text{CS}} \approx 7$ ppm, which overlaps strongly with the resonance at 0 ppm. Its intensity remains negligibly small in the low alkali range, but increases rapidly as x approaches 0.5 (see Figure 6 and the discussion below).

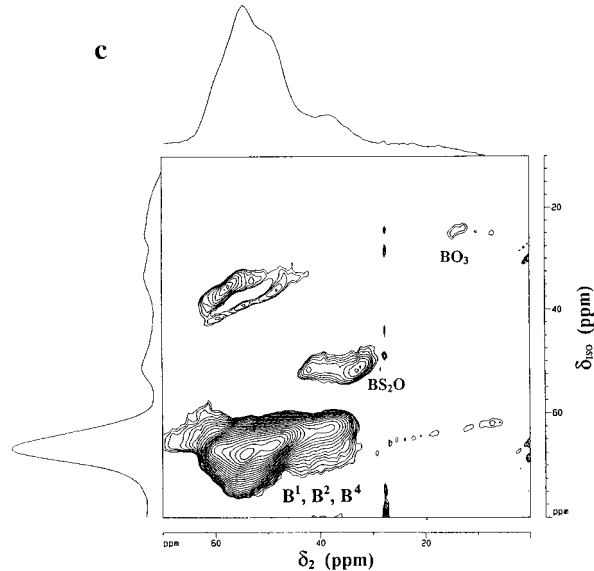
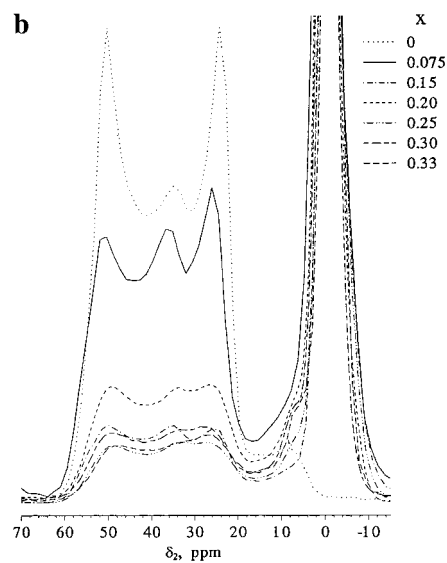
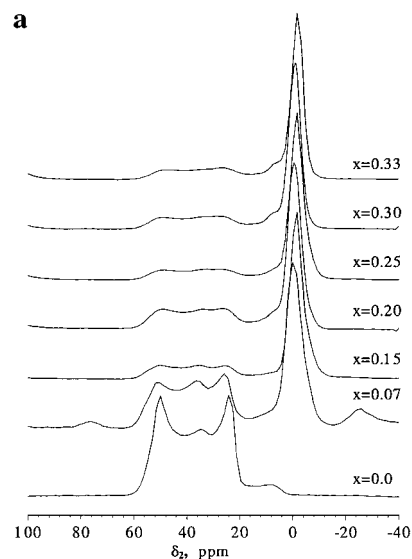


Figure 5. ^{11}B NMR spectra of $x\text{Na}_2\text{S} + (1-x)\text{B}_2\text{S}_3$ glasses in the low alkali glass forming range ($0 \leq x \leq 0.33$) obtained at 5.9 T: (a) under MAS displayed with the same height of the peak representing BS_4 units, (b) same as (a) but with the BS_3 resonance highlighted and normalized with respect to $v\text{-B}_2\text{S}_3$ ($x = 0$), (c) pure absorption phase MQMAS spectrum taken at 9.4 T for the glass formed at $x = 0.2$.

(43) Bray, P. J.; O'Keefe, J. G. *Phys. Chem. Glasses* **1963**, *4*, 37.

(44) Bray, P. J. *J. Non-Cryst. Solids* **1985**, *73*, 19.

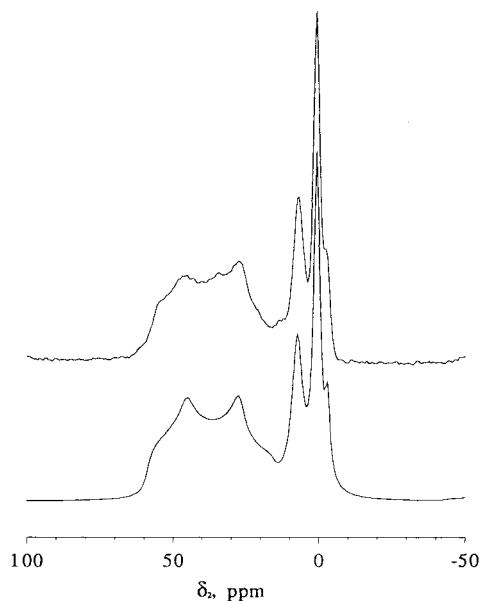


Figure 6. Experimental and simulated ^{11}B MAS NMR spectra of glassy metathiorate at 5.9 T.

Figure 5c shows the ^{11}B MQMAS NMR spectrum measured at 9.4 T for the glass with $x = 0.2$. Note that BS_4 resonance is not displayed in this spectrum. As in the case of vitreous B_2S_3 reported earlier,¹² the powder pattern representing BS_3 units is narrowed in the isotropic dimension; however, various trigonal sites still remain unresolved. Most likely, B^1 , B^2 , and B^4 sites contribute to this resonance. The oxygen contamination of this sample involves primarily BS_2O , but a very small amount of BO_3 units is also observed.

1.4. Glass with Metathiorate Composition ($x = 0.5$).

Figure 6 shows the ^{11}B MAS NMR spectrum and its computer simulation for the $x\text{Na}_2\text{S} + (1-x)\text{B}_2\text{S}_3$ glass with $x = 0.5$. At this composition glass is not readily formed, and the NMR spectra show that the obtained structure is more complex than that of the corresponding polycrystalline sample (Figure 3a). The integration of the spectrum in Figure 6 shows that 46% of boron atoms in this sample are tetrahedrally coordinated. Furthermore, at least three different types of BS_4 groups can be distinguished: a resonance at 7 ppm that includes 18% of the boron sites, and two narrow resonances at 1 and -3 ppm with relative intensities of 24% and 4%, respectively. Most likely, the last two peaks represent boron atoms in two dithiorate-like structures that differ slightly due to the presence of the metathioroxyl rings and nonbridging sulfur atoms. The resonance at 7 ppm must also be associated with the BS_4 units, although in a somewhat different environment than in dithiorate. We propose that this resonance represents the BS_4 groups with a nonbridging sulfur resulting from the decomposition of dithiorate.

The powder pattern of the BS_3 units in Figure 6 closely resembles that of Figure 3a for $x = 0.50$, which was assigned to metathioroxyl rings $\text{B}_3\text{S}_6^{3-}$. The computer simulation of this part of the spectrum yielded $C_Q = 2.51(0.02)$ MHz, $\eta_Q = 0.39(0.09)$, and $\delta_{\text{CS}} = 62(2)$ ppm, which agrees reasonably well with the data obtained for the corresponding polycrystalline phase. A small contribution from another BS_3 species is present in this sample as well, similar to resonance B^5 in Figure 3d.

1.5. High Alkali Glasses ($0.5 \leq x \leq 0.8$). The ^{11}B NMR spectra of glasses with $0.55 \leq x \leq 0.8$ (Figure 7) show a continuous conversion of the metathioroxyl rings ($\text{B}_3\text{S}_6^{3-}$) into orthothiorate units. Note that in the glass-forming range

Table 1. Assignments of the ^{11}B Resonances in $x\text{Na}_2\text{S} + (1-x)\text{B}_2\text{S}_3$

resonance	δ_{CS} (ppm) ^a	assignment
B^1	61(± 1)	borosulphol $\text{B}_3\text{S}_6^{3-}$ ring
B^2	64(± 1)	4-membered ring in B_2S_3
B^{3b}	from $-3(\pm 1)$ to $7(\pm 1)$	BS_4
B^4	60(± 1)	metathioroxol $\text{B}_3\text{S}_6^{3-}$ ring
B^5	64(± 3)	unknown, see Section 1.2.2
B^6	67(± 3)	BS_3^{3-} in orthothiorate
B^7	71(± 3)	BS_3^{3-} in orthothiorate
BO_3	17(± 3)	BO_3 ; O contamination
BSO_2	31(± 3)	BSO_2 ; O contamination
BS_2O	44(± 3)	BS_2O ; O contamination

^a The uncertainties for chemical shifts obtained via simulations of the anisotropic spectra are ± 1 and ± 2 ppm for polycrystalline and glassy samples, respectively; the values obtained from the graphical analysis of MQMAS spectra are accurate to within ± 3 ppm. ^b Several distinguishable BS_4 sites were found, as discussed in Sections 1.2, 1.3, and 1.4.

$0.5 \leq x \leq 0.65$, the MAS spectra of the BS_3 units are relatively broad and featureless. This is due to the overlap of the highly asymmetric powder patterns from the $\text{B}_3\text{S}_6^{3-}$ rings and from the boron atoms in BS_3 positions produced by addition of an increasing number of Na_2S molecules, such as pyrothiorate. However, at $x \geq 0.75$ the spectrum becomes relatively simple, and consists primarily of one powder pattern similar to that found in a polycrystalline orthothiorate (see Figure 3a). Similar behavior was observed in the IR spectra of these glasses.¹⁰

The BS_4 units are still present in all spectra of Figure 7, although their intensity gradually decreases. The peak at 7 ppm shows its maximum intensity at $x = 0.5$ and disappears at $x = 0.7$. Surprisingly, a small concentration of the dithiorate-like units remains in the glasses even at $x \geq 0.7$.

A ^{11}B MQMAS spectrum of the glass with $x = 0.6$, taken at 9.4 T is shown in Figure 7b. Although the resonances from various BS_3 units overlap strongly in the isotropic dimension, the main resonance is identical to the one that was previously labeled B^5 (see Section 1.2.2). In addition, a weakly resolved shoulder in a position similar to the BS_3^{3-} units in orthothiorate (B^6) is distinguished in the downfield portion of the spectrum. The use of a different magnetic field would allow for a better distinction between the different trigonal units. Again, the BS_2O , BSO_2 , BO_3 , and BS_4 species are detected as well-separated peaks in the two-dimensional spectrum.

The results of the above sections are summarized in Table 1, where the list of ^{11}B resonances is given along with the corresponding chemical shifts and interpretation.

1.6. N_4 Fraction. Earlier static ^{11}B NMR studies of glassy materials examined the composition dependence of the N_4 fraction, which accounts for the relative intensity of borons in a tetrahedral environment. The determination and analysis of the evolution of N_4 fraction versus glass composition (e.g., alkali content) facilitated the construction of structural models for these materials. This evolution was often correlated with the change in thermal and mechanical properties of glasses. For example, the N_4 fraction was intensely investigated in earlier studies of borate glasses, as the traditional static ^{11}B cw NMR is well suited for this measurement.^{22,43,45} Figure 8 shows the N_4 fraction of all $x\text{Na}_2\text{S} + (1-x)\text{B}_2\text{S}_3$ samples studied in this work obtained from the integrated BS_4 and BS_3 intensities in the ^{11}B MAS spectra taken at 5.9 T. Also plotted in Figure 8 are the earlier data of Sills et al.²² measured at 1.6 T with the static NMR method. The results are in good agreement and demonstrate

(45) Eckert, H. *Prog. NMR Spectrosc.* **1992**, *24*, 159, and references therein.

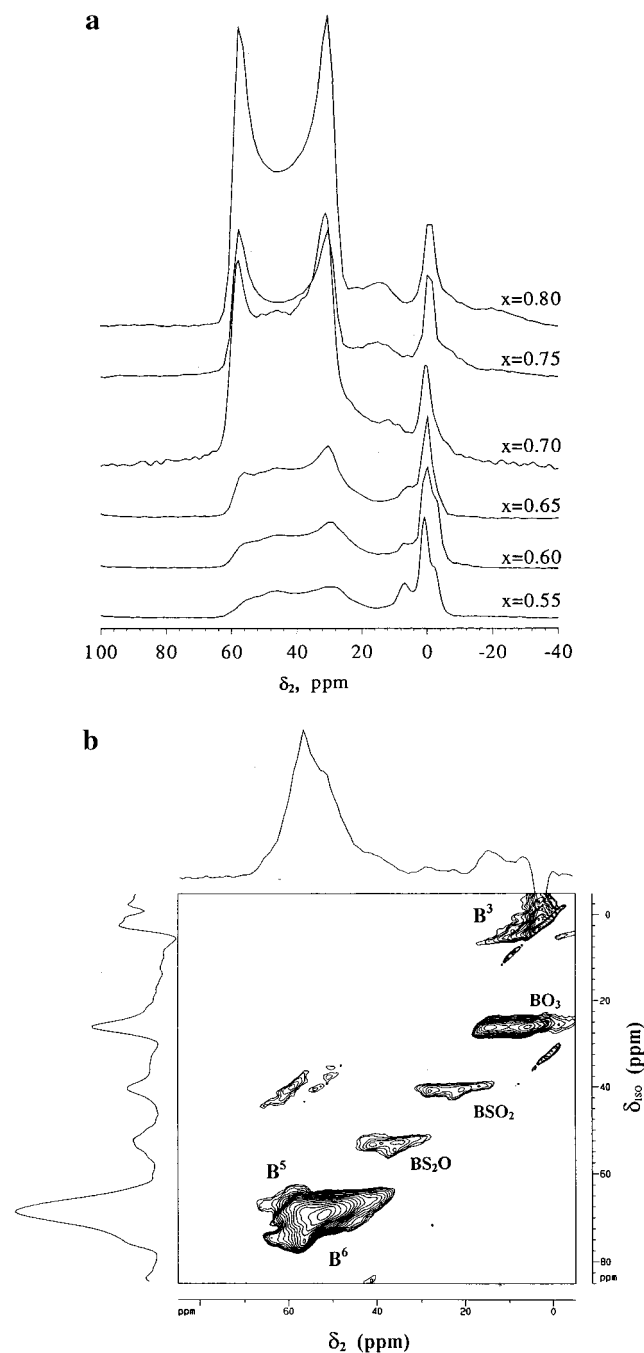


Figure 7. (a) ^{11}B MAS NMR spectra at 5.9 T of $x\text{Na}_2\text{S} + (1-x)\text{B}_2\text{S}_3$ glasses in the high alkali glass forming range ($0.55 \leq x \leq 0.80$). (b) ^{11}B MQMAS NMR spectrum taken at 9.4 T for the glass formed at $x = 0.6$.

the overall evolution of $\text{BS}_3 \rightarrow \text{BS}_4 \rightarrow \text{BS}_3$ units described in the previous sections. We note that for $x < 0.2$ the $N_4(x)$ curve can be well fitted with $4x/(1-x)$, which corresponds to the initial conversion of 8 BS_3 units per Na_2S added. The initial slope of $x/(1-x)$, corresponding to conversion of two BO_3 to BO_4 units per M_2O added, was found in an earlier study of alkali borate glasses.⁴⁴ Thus, our data strongly suggest that the models invoked by Krogh-Moe⁴⁶ for the forming of borate glasses are not operable in the $x\text{Na}_2\text{S} + (1-x)\text{B}_2\text{S}_3$ system. We note that at a conversion rate of $4x/(1-x)$, N_4 would reach 1 at $x = 0.2$. This result implies that the initial addition of Na_2S does not simply introduce the dithioborate units into the glass structure, because such a process would follow the $2x/$

(46) Krogh-Moe, *J. Phys. Chem. Glasses* **1965**, 6, 46.

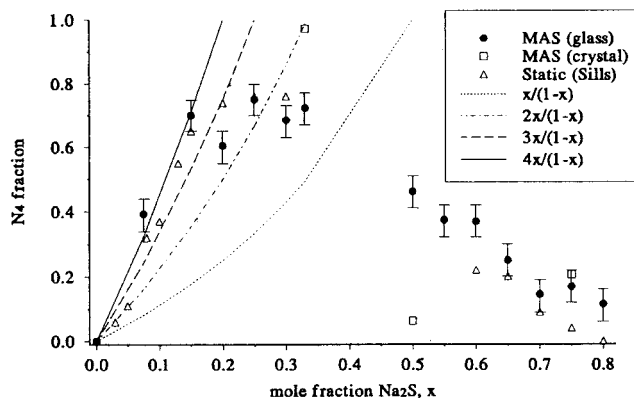


Figure 8. The N_4 fraction determined by ^{11}B MAS NMR spectra at 5.9 T and ^{11}B static NMR at 1.95 T (from earlier work by Sills et al.²²).

$(1-x)$ curve and result in complete conversion at $x = 0.33$. As noted earlier, while dithioborate-type units appear to be the dominant structure at $x = 0.33$, the $x\text{Na}_2\text{S} + (1-x)\text{B}_2\text{S}_3$ glass retains a substantial concentration of the BS_3 units. Similarly, at meta- and orthothioborate compositions the glasses still contain considerable amounts of the BS_4 units. To better understand the intermediate-range order and to uncover the structural changes occurring upon addition of Na_2S , the ^{11}B MQMAS NMR of all samples should be performed in concert with quantitative numerical analysis of the basic MAS spectra.^{12,30} Such an analysis would allow for separate monitoring of all structural units described in the previous sections, including the oxygen-containing impurities which skewed the accuracy of the data in Figure 8.

2. ^{23}Na NMR. 2.1. Polycrystalline $x\text{Na}_2\text{S} + (1-x)\text{B}_2\text{S}_3$.

Figure 9a shows the ^{23}Na MAS NMR spectra of Na_2S and the polycrystalline samples taken at 5.9 T. A single narrow resonance at around 50 ppm is observed in Na_2S , which was studied in its "as received" state. This result is consistent with the expected antifluorite structure in which each S anion is surrounded by eight Na cations located at the corners of a cube and each Na cation by four S anions at the corners of a tetrahedron.⁴⁷

The ^{23}Na MAS NMR spectrum of dithioborate shows a single symmetric 2.2 kHz wide (fwhm) resonance at ~ -50 ppm. A similar experiment performed at -110 °C produced a wider (4.3 kHz) and slightly asymmetric resonance that shifted to ~ -36 ppm. It is expected that the observed line width is determined by the second-order quadrupolar interaction, the distribution of chemical shifts, and the exchange processes. These contributions can be further influenced by motion. The chemical shift anisotropy broadening and homo- and heteronuclear ($^{11}\text{B}-^{23}\text{Na}$) dipolar couplings, which often affect the ^{23}Na NMR line width of glasses in the static samples,^{48,49} can be neglected under MAS at 10 kHz. Since we have not performed further investigations of the exact origin of the observed line changes, we can only speculate that they result from the change of sodium environment and its mobility. In particular, the temperature dependence of the resonance frequency is due to the quadrupolar induced shift resulting from the change of the equilibrium location of the Na^+ ions in the lattice of thioborate crystals, whereas the slowing down of their motion at lower temperatures causes the increased line width.

(47) Cotton, F. A.; Wilkinson, G. *Advanced Inorganic Chemistry*; John Wiley & Sons: New York, 1980.

(48) Emerson, J. F.; Bray, P. J. *J. Non-Cryst. Solids* **1994**, 169, 87.

(49) Gee, B.; Eckert, H. *Solid State Nucl. Magn. Reson.* **1995**, 5, 113.

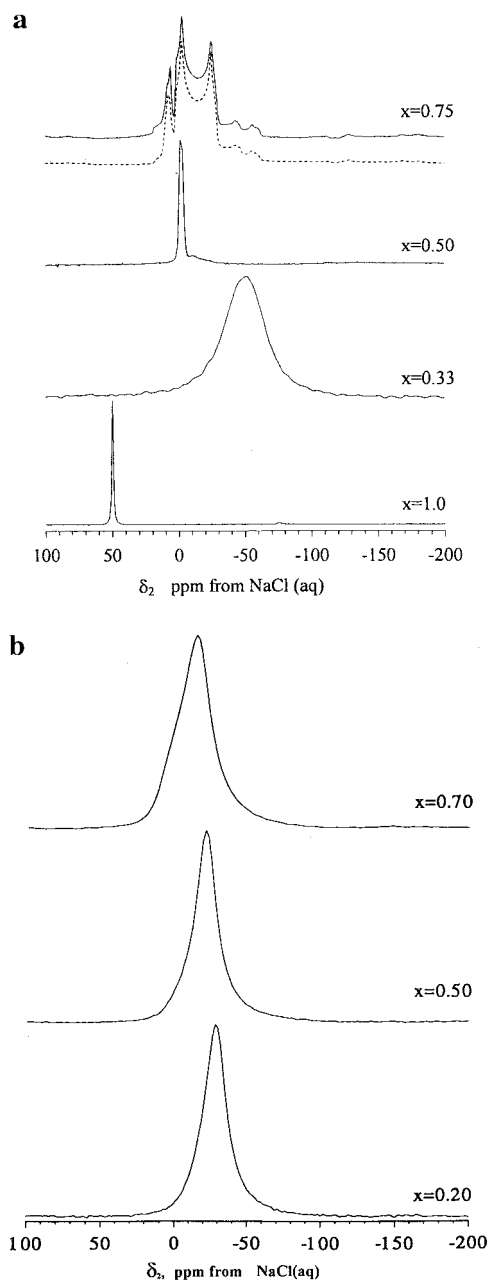


Figure 9. ^{23}Na MAS NMR spectra of $x\text{Na}_2\text{S} + (1-x)\text{B}_2\text{S}_3$ obtained at 5.9 T. (a) Polycrystalline compounds with $x = 0.33, 0.50, 0.75$, and 1. For $x = 0.75$, the dashed line represents the simulated spectrum. (b) Glasses formed at $x = 0.20, 0.50$, and 0.70 .

The spectrum of metathiorate ($x = 0.50$) shows an intense narrow line at ~ 0 ppm and a weak broad resonance at ~ -10 ppm. The slightly anisotropic line at 0 ppm is consistent with the single-crystal X-ray diffraction data, which showed that the Na^+ ions in $\text{Na}_3\text{B}_3\text{S}_6$ are positioned in a coordination sphere of seven S^- ions with bond distances between 0.297 and 0.342 nm.¹⁵ The assignment of the weak resonance at -10 ppm is not straightforward. Most likely its presence is associated with the structural impurities uncovered via MQMAS ^{11}B NMR.

The ^{23}Na MAS NMR spectrum of orthothiorate ($x = 0.75$) shows (at least) three different Na sites coordinated to non-bridging sulfur atoms, and could be well characterized with QUASAR (see dashed line in Figure 9a and Table 2).

Although the exact location of Na^+ cations in $3\text{Na}_2\text{S}\cdot\text{B}_2\text{S}_3$ is unknown, complete crystal structures of several analogous borate and thiorate compounds have been obtained from X-ray

Table 2. Parameters Obtained from ^{23}Na NMR Lineshape Simulation of Orthothiorate

site	rel intensity	δ_{CS} (ppm)	C_Q (MHz)	η_Q	line broadening (Hz)
Na^1	0.66(± 0.01)	8.0(± 0.1)	1.97(± 0.05)	0.16(± 0.01)	58(± 10)
Na^2	0.24(± 0.01)	18.7(± 0.1)	3.01(± 0.05)	0.83(± 0.01)	80(± 10)
Na^3	0.10(± 0.01)	11.2(± 0.1)	0.77(± 0.03)	0.61(± 0.03)	100(± 15)

diffraction data. For example, $\alpha\text{-Li}_3\text{BO}_3$ and Na_3BO_3 were shown to consist of almost planar BO_3^{3-} anions connected by Na^+ cations which occupy three types of inequivalent sites,^{50,51} whereas in orthothiorate Ti_3BS_3 the planar BS_3^{3-} triangles were connected by two types of crystallographically independent Ti^+ anions.¹⁷ Since the positions of all cations involved in these compounds exhibit a nonsymmetric arrangement of the neighboring atoms, we expect that sites Na^1 and Na^2 represent two distinct Na^+ ions in the Na_3BS_3 units that are strongly bound to sulfur on one side (see Figure 1) and loosely coordinated to the sulfur atoms in the neighboring units. The origin of the narrow resonance (site Na^3), which represents sodium in a more symmetric coordination environment, is at present unknown. Further studies involving ^{23}Na MQMAS and the experiments probing $^{11}\text{B}\text{-}^{23}\text{Na}$ and $^{23}\text{Na}\text{-}^{23}\text{Na}$ dipolar interactions are needed to better characterize the structure of orthoborates and orthothiorates.

2.2. Glassy $x\text{Na}_2\text{S} + (1-x)\text{B}_2\text{S}_3$. In contrast to most polycrystalline samples, all $x\text{Na}_2\text{S} + (1-x)\text{B}_2\text{S}_3$ glasses exhibit single broad ^{23}Na resonance lines. The static line width of ^{23}Na spectra varied with composition from ~ 2.5 kHz for $x = 0.5$ to ~ 4.5 kHz for $x = 0.7$, whereas magic angle spinning resulted in line narrowing by a factor of approximately two (to 1.1 and 1.8 kHz in these two samples, respectively). However, the second-order quadrupolar broadening appears insignificant in these samples, as the resolution could not be further improved by using MQMAS or DOR, which were attempted at 9.4 and 4.7 T, respectively, for the glass with $x = 0.55$ (spectra not shown).

It is noted that the spectra shift downfield with increasing Na^+ ion content (see the spectra for $x = 0.2, 0.5$, and 0.7 in Figure 9b). Assuming that the peak position is largely attributed to changes in chemical shift, this indicates that the average shielding is diminished upon addition of Na_2S . Similarly, smooth changes in the sodium peak position were recently observed in silicate glasses $[(1-x)\text{Li} + x\text{Na}]_2\text{O}\cdot 2\text{SiO}_2$.⁵² This result was interpreted as evidence of intimate and uniform mixing of the two alkali in the network structure which itself does not change significantly with x .⁵² However, the ^{11}B NMR showed that the structures of the thiorate glasses studied here change dramatically as a function of alkali content. For example, each of the glassy samples with $x = 0.2, 0.5$, and 0.7 consists of both BS_3 and BS_4 units and therefore contains at least two types of sodium sites which should be separable spectroscopically. Furthermore, the lack of change in the ^{23}Na NMR line width versus x is in contrast to the polycrystalline samples with similar composition (e.g., at orthothiorate composition the spectrum of the glassy sample is significantly narrower than that of the polycrystalline sample). Although the structural disorder may contribute to the ^{23}Na line width and to the absence of distinct features in the spectra of Figure 9b, the above observations suggest that the dynamical behavior

(50) Stewner, V. F. *Acta Crystallogr.* **1971**, B27, 904.

(51) Konig, V. H.; Hoppe, R. Z. *Anorg. Allg. Chem.* **1977**, 484, 225.

(52) Ali, F.; Chadwick, A. V.; Greaves, G. N.; Jermy, M. C.; Nagai, K. L.; Smith, M. E. *Solid State Nucl. Magn. Reson.* **1995**, 5, 133.

of Na⁺ ions is primarily responsible for the observed line shapes. Better insight into the dynamic processes involving Na⁺ ions can be gained from relaxation studies and low-temperature MQMAS experiments, which are beyond the scope of this work.

Conclusions

By employing high-speed ¹¹B and ²³Na MAS NMR methods in conjunction with the MQMAS NMR technique, we have examined the structural evolution of a polycrystalline and glassy alkali binary thioborate system $x\text{Na}_2\text{S} + (1 - x)\text{B}_2\text{S}_3$ in the range $0 \leq x \leq 0.8$. ¹¹B MAS NMR spectra of polycrystalline samples obtained with $x = 0, 0.5,$ and 0.75 were representative of crystallographically known structures and the NMR line shape parameters were determined by computer simulations. A polycrystalline phase was also obtained for $x = 0.33$ and its structure is proposed based on the NMR spectrum. With this structural information as a reference, the evolution of the SRO of the basic network structures in a wide range of glass compositions was probed by ¹¹B MAS and MQMAS NMR of selected samples. The room temperature study of the sodium coordination environment by ²³Na MAS NMR was less informative due to motional averaging and the inherent disordered arrangement of Na⁺ ions.

It is suggested that a systematic MQMAS-based investigation combined with quantitative numerical analysis of the MAS spectra will lead to better understanding of the intermediate-range order in these materials. Finally, the use of CPMQMAS and/or MQ-REDOR experiments for studying connectivities^{53,54} between ²³Na and ¹¹B spins may lead to new insights.

Acknowledgment. This research was supported at Ames Laboratory by the U.S. Department of Energy, Office of Basic Energy Sciences, Division of Chemical Sciences, under Contract No. W-7405-Eng-82 and by the National Science Foundation, Division of Materials Research, Grant No. NSF-DMR 94-020651. The authors thank Dr. H. Eckert, Dr. H. F. Franzen, and D. P. Lang for valuable discussions. One of the authors (J.-W.H.) was supported in part by Taegu University Research Grant 1997.

JA9800481

(53) Pruski, M.; Lang, D. P.; Fernandez, C.; Amoureux, J. P. *Solid State Nucl. Magn. Reson.* **1977**, *7*, 327.

(54) Fernandez, C.; Lang, D. P.; Amoureux, J. P.; Pruski, M. *J. Am. Chem. Soc.* **1998**, *120*, 2672.